

Nanocellulose-silica polyethersulfone hybrid composite stabilized lipase for esterification

Cite as: AIP Conference Proceedings 2155, 020017 (2019); <https://doi.org/10.1063/1.5125521>
Published Online: 06 September 2019

Nursyafiqah Elias, Lau Woei Jye, and Roswanira Abdul Wahab



View Online



Export Citation

ARTICLES YOU MAY BE INTERESTED IN

[Proximate analysis and bioactivity study on acoustically isolated *Elaeis guineensis* leaves extract](#)

AIP Conference Proceedings 2155, 020001 (2019); <https://doi.org/10.1063/1.5125505>

[Ultrasound-assisted extraction of polyphenols from pineapple skin](#)

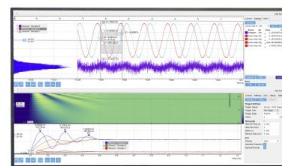
AIP Conference Proceedings 2155, 020002 (2019); <https://doi.org/10.1063/1.5125506>

[Fire-retardancy of wood coated by titania nanoparticles](#)

AIP Conference Proceedings 2155, 020022 (2019); <https://doi.org/10.1063/1.5125526>

Challenge us.

What are your needs for periodic signal detection?



Zurich
Instruments



Nanocellulose-silica polyethersulfone hybrid composite stabilized lipase for esterification

Nursyafiqah Elias^{1,2, a)}, Lau Woei Jye^{3, b)} and Roswanira Abdul Wahab^{1, 2, c)}

¹ Department of Chemistry, Faculty of Science, Universiti Teknologi Malaysia, 81310 UTM Johor Bahru, Malaysia

² Enzyme Technology and Green Synthesis Group, Faculty of Science, Universiti Teknologi Malaysia, 81310 UTM Skudai, Johor, Malaysia

³ Advanced Membrane Technology Research Centre (AMTEC), Universiti Teknologi Malaysia, 81310, Skudai, Johor, Malaysia

^{c)} Corresponding author: roswanira@kimia.fs.utm.my

^{a)} syafiqah.nse@gmail.com

^{b)} lwoeijye@utm.my

Abstract. An alternative environmentally benign support was prepared from nanocrystalline silica (SiO₂), and cellulose (NCC) acquired from oil palm fronds leaves (OPFL) for incorporation with polyethersulfone (PES). The resultant PES-SiO₂-NCC support was then used for covalent immobilization of *Candida rugosa* lipase (CRL/PES-SiO₂-NCC). FTIR-ATR spectral data of SiO₂-NCC indicated that NCC was hydrogen-bonded to SiO₂ based on the characteristic wavenumbers at 1735 cm⁻¹ and 1650 cm⁻¹ for NCC, 1732 cm⁻¹ and 1657 cm⁻¹ for SiO₂, alongside decreased peak intensity and the overall downshifted wavenumbers, respectively. X-ray diffractograms of NCC and SiO₂ showed crystallinity indices of 68% and 70%, respectively, implying their crystalline nature. The CRL/ PES-SiO₂-NCC biocatalyst yielded pentyl valerate as high as 78.3% after 2 h using a 0.02 cm membrane size and 5% (w/v) incorporation of SiO₂-NCC but in the absence of the pore former, PVP K30. The findings invariably envisage the biocompatibility of NCC and SiO₂ derived from OPFL as a hybrid nano-filler to prepare the PES-SiO₂-NCC composite for lipase immobilization.

INTRODUCTION

Biocatalysis has significantly gained popularity in the industrial biotechnology sector in the last decade following the emergence of “Green Chemistry” as an alternative to the less environmentally-friendly conventional chemical route. Currently, an assortment of bio-enzymes is available to replace the chemical processes used in industries such as textiles, food, and beverages, cosmetics, pharmaceuticals as well as bulk and fine chemical synthesis [1-3]. Lipases (triacylglycerol hydrolases, EC.3.1.1.3) is the third most important group of enzymes used in many industrial manufacturers. Their excellent catalytic features, for instance, specificity, regio- and enantioselectivity and ability to catalyze in organic solvents [4], in addition to their natural ability to hydrolyze carboxylic ester bonds has seen them being used for mediating different kinds of biotransformation reactions [5]. Among others, *Candida rugosa* lipase (CRL) is a commonplace enzyme for catalyzing reactions such as oil hydrolysis, transesterification, esterification, and interesterification [5-7].

However, it best that lipases are utilized in an immobilized state, in most part, for increased robustness, as well as to enable easy catalyst recovery after completion of reactions, alongside immediate reuse in multiple catalytic cycles [8]. The covalent attachment of lipases to the surface of the support is the more preferred method following the formation of strong bonds between the lipase and support [9]. Typically, immobilized enzymes show greater activity, selectivity, and stability, in organic media in comparison to their free counterpart [10].

In this study, CRL was covalently bound onto a hybrid nanocellulose-silica-reinforced polyethersulfone (PES) membrane to improve the stability and reusability of the lipase. The resultant CRL/PES-SiO₂-NCC nano biocatalyst was evaluated for efficacy in catalyzing an esterification reaction to

produce pentyl valerate, via the esterification of pentanol and valeric acid. This worth noting here that the proposed ester has been increasingly used as an alternative biofuel additive in compression ignition engines such as diesel engines. The objective of this study was to identify the best parameters to prepare the PES-SiO₂-NCC nanocomposite for CRL immobilization, to ensure the lipase catalyzes the maximum conversion degree of pentyl valerate. Our study complements existing efforts worldwide to introduce lean carbon energy sources, for example, bioethanol obtained by fermentation of sugars or biodiesel by hydrolysis of vegetable oil [11, 12], to minimize the impact of fossil fuel utilization on the environment. Moreover, valeric biofuels are found more compatible as transportation fuels for both gasoline and diesel engines than run on other types of biofuels.

MATERIALS AND METHODS

Chemicals and Instrumentations

Candida rugosa lipase (CRL) (≥ 700 U/mg), polyethersulfone pellet (3 mm nominal granule size), pentanol (> 99% purity), valeric acid (> 99% purity) and phenolphthalein were purchased from Sigma-Aldrich Ltd (St. Louis, USA). The chemicals were of analytical grade and used without further purification while distilled water was prepared in our laboratory.

Isolation of silica (SiO₂)

Silica was isolated and purified from raw oil palm frond leaves (OPFL) using a previously developed method [13], with some modifications. OPFL powder (50.0 g) was dissolved in 1.0 M HCl (500 mL) and heated in an oil bath at 100 °C under continuous stirring for 2 h (400 rpm). The dispersion was left to cool at ambient temperature, and the supernatant was decanted. The wet dispersed powder was washed several times with copious amounts of ultrapure water till neutrality. The dispersed powder was filtered and dried in an oven for 24 h at 80 °C. Next, the treated samples (OPFT) were placed in silica crucibles (150 mL) and calcined for 9 h in a 600 °C preheated furnace (Nabertherm R; Germany). The resultant silica (SiO₂) were collected and kept in screw-capped bottles at room temperature until further use.

Isolation of nanocellulose (NCC)

OPFL were manually sorted, washed, and dried before grinding into a fine powder followed by storing in sealed plastic bags room temperature. The OPFL powder (20 g) was refluxed at 85 °C in a mixture of acetic acid, sodium chlorite and distilled water (1.2 mL: 6 g: 600 mL). The subsequent holocellulose (HC) product was further isolated using five repeated treatments with a mixture of acetic acid and sodium chlorite at 1 h intervals. The reaction mixture was further heated at 70 °C for overnight with constant stirring. The HC product was filtered and repeatedly rinsed with ultrapure water till neutrality before drying in an oven at 70 °C overnight.

The subsequent alkali treatment on the produced HC was important for removing the remaining hemicelluloses and lignin. About 2 g oven dried weight of the extracted OPF was added into 30 mL of sodium hydroxide solution (17%, w/v) and was stirred (200 rpm) for 5 h at room temperature. Next, ultrapure water was added into the solution, and the mixture was stirred for a further 10 min. The cellulose (CS) product was filtered and thoroughly rinsed in copious amounts of ultrapure water till neutrality before drying in a 70 °C oven overnight.

Next, 10 g of dried CS product was hydrolyzed in 100 mL sulfuric acid solution (9 M) at room temperature for 5 h under continuous magnetic stirring. The reaction was halted by adding fresh ultrapure water followed by repeated washing process to remove the acid. The resulting suspension was first frozen, followed by lyophilization to obtain the dried nanocellulose (NCC).

Characterization of extracted SiO₂ and NCC

The extracted SiO₂ and NCC, as well as SiO₂-NCC nanoparticles, were characterized by using Fourier Transform Infrared spectroscopy: attenuated total reflection (FTIR-ATR) and x-ray diffraction analysis (XRD) to observe their physicochemical characteristics after the chemical treatments.

The spectral data of the samples were in the one-bounce ATR mode using a Spectrum 100 FTIR spectrometer (Perkin-Elmer Inc., Norwalk, CT, USA). A small amount of each sample was placed on

Diamond/ZnSe crystal plate (Perkin-Elmer), and the spectral data was obtained between the spectral region 4000–500 cm⁻¹ at room temperature.

The XRD analysis patterns were collected using a powder X-ray diffractometer (D/max 2200, Rigaku, Japan) that equipped with Cu K α radiation source ($\lambda = 0.154$ nm) operating at 40 kV and 30 mA. The XRD pattern was recorded over the angular range $2\theta = 10^\circ - 40^\circ$ with a $10^\circ \text{ min}^{-1}$ step increment. The crystallinity index (I_c) was calculated from the heights of the 002 peak and the intensity minimum between the 002 (I_{002} , $2\theta = 21^\circ$) and 101 (I_{101} , $2\theta = 12^\circ$) peaks (I_{am} , $2\theta = 15^\circ$) using the Segal method (Segal et al., 1959) as shown in Equation 1. I_{002} signifies both crystalline and amorphous material, whereas I_{am} denotes the amorphous material.

$$I_c = \frac{I_{002} - I_{am}}{I_{002}} \times 100 \quad (1)$$

Fabrication of SiO₂-NCC nanoparticles

Surface functionalization of SiO₂ with NCC was done via ultrasonic irradiation technique. Dried SiO₂ (0.05 g) was dispersed in 25 mL dimethylsulfoxide solution followed by a 20 min sonication on a VCX130 ultrasonicator (UK), before 0.10 g of NCC was added to the mixture and was sonicated for a further 45 min. The mixture was filtered and dried at 80 °C for more than 24 h to obtain the SiO₂-NCC nanoparticles.

Fabrication of PES-SiO₂-NCC composite

Optimization of the method to prepare the PES-SiO₂-NCC hybrid composite was monitored through the effect of pore former (PVP K30), the percentage of SiO₂-NCC nanoparticles and the size of the composite for the esterification production of pentyl valerate. The dope solution was first prepared by adding PVP K30 if any into NMP followed with stirring at 100 rpm till homogeneity. This was followed by the addition of the SiO₂-NCC nanoparticles (0.1, 1.5, 3.0 and 5.0%) into the mixture, followed by sonication for 1 h to homogeneously disperse nanomaterial in the solvent. Pre-dried PES polymer pellets were then added into the mix, and the mixture was continuously stirred for a further 1 h until a homogenous dope solution was obtained. The prepared dope formulations are summarized in Table 1. The nanoparticle loading percentage was determined by the total weight of neat membrane dope solution, all of which was fixed at 100% (i.e., 0.1%), where SiO₂-NCC of 100 g is equivalent to 0.1 g of SiO₂-NCC into 100 g of dope solution formula.

PES-SiO₂-NCC composite with a thickness of 100 ± 10 μm was cast on a clean and dry glass plate using a glass rod. The casted composite was then immersed into a water coagulation bath at room temperature to initiate phase inversion. The formed membrane was peeled off from the glass plate surface and then transferred into another clean water bath. All the casted membranes were kept in a water bath for at least 24 h to remove the polyvinylpyrrolidone (PVP) and residual solvent. The membranes were then dried at room temperature before they were cut into various sizes (0.02 cm, 0.05 cm, 1 cm, 2 cm) prior to CRL immobilization.

TABLE 1. Dope formulation of PES neat and PES-SiO₂-NCC nanocomposite membranes.

Dope	PES (wt%)	PVP K30 (wt%)	SiO ₂ -NCC (wt%)	NMP (wt%)	Total weight (wt%)
PES-neat	15	1.5	-	83.5	100
PES-SiO ₂ -NCC 0.1%	15	1.5	0.1	83.4	100
PES-SiO ₂ -NCC 1.5%	15	1.5	1.5	82.0	100
PES-SiO ₂ -NCC 3.0%	15	1.5	2.0	81.5	100
PES-SiO ₂ -NCC 5.0%	15	1.5	5.0	78.5	100

CRL immobilized onto PES-SiO₂-NCC composite

The PES-SiO₂-NCC was impregnated in an aqueous solution of glutaraldehyde (2.5%) for 4 h at room temperature. The composite was removed from the glutaraldehyde solution and washed with ultrapure water and left to dry in a desiccator overnight. Next, the PES-SiO₂-NCC composite was then immersed in 20 mL CRL solution (10 mg/mL) in 0.05 M phosphate buffer of pH 7 for 4 h at room temperature. The obtained CRL/PES-SiO₂-NCC were removed from the lipase solution and washed with phosphate buffer (0.05 M, pH 7) to remove any unbound lipase from the membrane surface. The membrane was filtered and dried overnight in a desiccator before storing at 4 °C until further usage.

Synthesis of Pentyl Valerate Catalyzed by CRL/PES-SiO₂-NCC Composite

Esterification of pentyl valerate was initiated using pentanol (Sigma Aldrich, 99%) and valeric acid (Sigma Aldrich, 99%) (molar ratio of acid to alcohol; 1:2) in the presence of cyclohexane as the solvent (Sigma Aldrich, 99%), prior to adding the free CRL or CRL/PES-SiO₂-NCC (3 mg/mL). Each reaction mixture was incubated in an oil bath at 50 °C before 2 mL of ethanol was added as the quenching agent. The solution was then directly titrated using 0.2 M NaOH. A 200 µL aliquot of each reaction mixture was taken at the beginning of the reaction, and every 1 h interval. The sample mixture was titrated using 0.2 M NaOH with phenolphthalein as the indicator. The blank containing acid and alcohol devoid of the enzymes were titrated to determine the total acid content of the reaction mixture. The synthesized pentyl valerate was expressed in terms of conversion (%), i.e., percent of valeric acid converted over the total acid in the mixture. The conversion (%) was calculated according to prescribed Equation 2:

$$\%Conversion = \left[\frac{V_0 - V_t}{V_0} \right] \times 100 \quad (2)$$

Where; V₀ = volume of NaOH at initial time (t = 0); V_t = volume of NaOH at each hour (t = t₁, t₂, t₃, ...). Each assessed factor that yielded the highest percent conversion of pentyl valerate was considered as the optimum and subsequently applied in the following investigations.

RESULTS AND DISCUSSION

Characterization of extracted SiO₂ and NCC

In this study, SiO₂ and NCC obtained from the OPFL were analyzed using FTIR: ATR spectroscopy to evaluate the presence of lignocellulosic compounds functional groups after the chemical treatments (Figure 1). Figure 1a reveals a broad and intense band in the region of 3321 cm⁻¹ were attributed to the O-H stretching vibrations of cellulose, hemicellulose, and lignin [14, 15] while a peak at 2903 cm⁻¹ corresponded to the -CH₂ stretching vibrations. The peak at 1650 cm⁻¹ was consistent with the O-H bending of the bound water in the cellulose structure, as a result of strong interactions between cellulose and water [15, 16]. The absence of peaks in the region of 1739 cm⁻¹ and 1538 cm⁻¹ normally ascribed to the C=O and C=C stretching vibrations conveyed that hemicellulose and lignin were successfully removed from the biomass by the chemical treatments. Notably, the intensity of a peak that emerged around 1012 cm⁻¹ was increased after each chemical treatment, and this was indicative of the qualitative increase in the degree of order of NCC (Figure 1a). The spectra are seen here supported the successful conversion of native cellulose I to cellulose II following the chemical treatments.

In contrast, the broad peaks at 3405 cm⁻¹ for SiO₂ was attributed to -OH stretching vibrations whereas the less prominent peaks at 1657 cm⁻¹ were assigned to -OH bending vibrations, both of which originated from the silanol (Si-OH) groups and trapped water molecules. The peaks below 1400 cm⁻¹ in the spectrum were due to the different vibration modes of SiO₂. The strong absorption peak observed at 1046 cm⁻¹ was attributed to the asymmetric stretching of the siloxane group (Si-O-Si), respectively (Figure 1b). The results seen here are similar to as previously described by another study for siloxane bonds from risk husk and olive stones [17, 18].

The absorption peaks for the asymmetric vibration of Si-O bonds in the structure of SiO₂-NCC (Figure 1c) appeared at 1068 cm⁻¹ while a peak at 800 cm⁻¹ was attributed to the vibration of Si-OH. A broad peak at 3334 cm⁻¹ was ascribed to the -OH of adsorbed water on the surface of the nanoparticles, whereas a peak at 2911 cm⁻¹ represented the C-H bending of a methyl group in the cellulose structure. Most importantly, the spectra indicated the successful fabrication of SiO₂-NCC support, as can be seen in Figure 1c, which showed the presence of characteristic peaks for both SiO₂ and NCC.

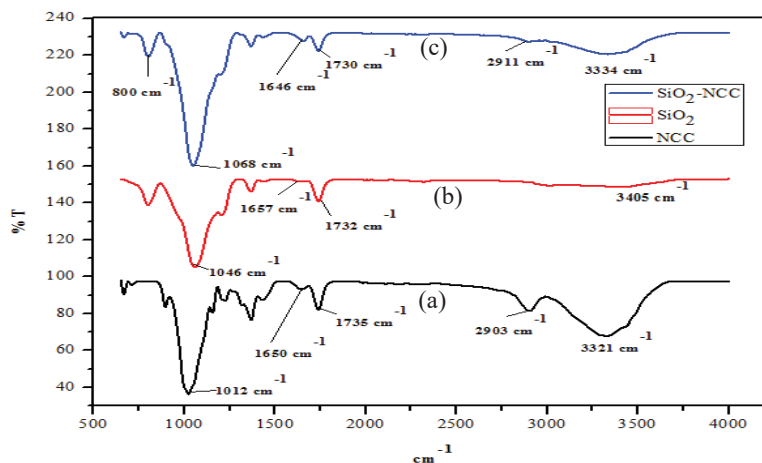


FIGURE 1. FTIR: ATR spectra of a) SiO₂-NCC, b) SiO₂ and c) NCC

Figure 2 shows the diffractograms for SiO₂, NCC, and SiO₂-NCC nanoparticles. The diffractograms indicated the major intensity peak was located at a 2θ value of 21° , directly related to the crystalline structure of cellulose I [19], while the amorphous part was characterized by the low-intensity peak at a 2θ value of 12° , as indicated by International Centre for Diffraction Data (ICDD) (JCPDS file no. 00-056-1718). The estimated crystallinity index of NCC after the chemical extraction was 68%, thus supported the successful removal of the amorphous non-cellulosic parts from the biomass (Figure 2a). The outcome seen here was consistent with similar studies on NCC preparations [20-22]. The presence of a doublet and sharp peak at $2\theta = 20^\circ$ and $2\theta = 21^\circ$ were indicative of the conversion of native cellulose I to cellulose II. Based on the results, this study suggested that the chemical treatment employed here was adequate and removed the majority of the amorphous materials from the OPFL powder.

In contrast, two major mineral phases [minehillite; $K_3Ca_{28}Zn_4Al_4Si_{40}O_{112}(OH)_{16}$] and [cristobalite; SiO₂] were identified in addition to amorphous materials was attributed to the decline of alkali earth metals concentration from the biomass that establishes by these minerals. The diffractogram for SiO₂ is amorphous in nature, which did not show any sharp diffraction peaks (Figure 2b) while the major component was cristobalite which corresponds to the SiO₂ as earlier reported by [17] and [23], with crystallinity index of 70%. Thus, this study suggested that the acid treatment successfully remove the other components, and the resulting silica becomes more evident following acid treatment of OPFL. The diffractogram of SiO₂-NCC consists of two-phase structures from the combination of NCC and SiO₂ properties, with lower crystallinity index (56%) (Figure 2c).

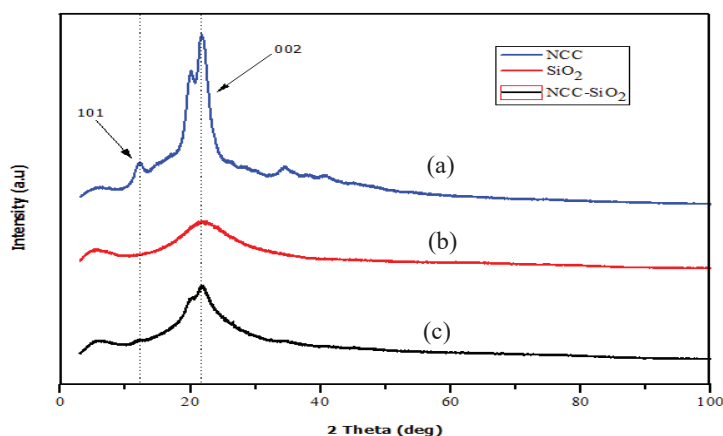


FIGURE 2. X-ray diffractograms of extracted a) NCC, b) SiO₂ and c) SiO₂-NCC from different chemical treatments.

Optimization of Membrane Fabrication

Effect of PVP K30

In this study, the effect of PVP K30 as the pore-forming agent was investigated for the conversion of pentyl valerate catalyzed by the biocatalyst CRL/PES-SiO₂-NCC (Figure 3). Polyethersulfone (PES) polymer was chosen as the membrane owing to its beneficial properties such as excellent chemical resistance and thermal stability, alongside a wide pH tolerance [24]. Results revealed that the highest conversion of pentyl valerate was achieved when CRL/PES-SiO₂-NCC was employed in the absence of PVP. This was followed by CRL/PES-SiO₂-NCC with PVP that afforded percent conversions of 66.8% and 55.6%, respectively (Figure 3).

The results indicated that more pentyl valerate was produced with the incorporation of SiO₂-NCC nanofiller into the PES membrane in the absence of PVP. This is consistent with a previously described effect, in which the addition of PVP increases the membrane hydrophilicity with the use of lower PES concentration [24]. However, this study found that the incorporated hydrophilic nanofiller into the hybrid composite was advantageous in activating CRL to catalyze higher conversion degree of pentyl valerate, without the presence of PVP into the membrane. CRL/PES-SiO₂-NCC with the incorporation of PVP (1.5%) catalyzed a comparable esterification production of the ester at 55.6% in just 2 h (Figure 3). Hence, it appeared that the SiO₂-NCC nanofiller played an important role in yielding a more biocompatible PES-SiO₂-NCC support for immobilization and activation of CRL. This consequently led to the improved conversion degree of pentyl valerate by the immobilized CRL.

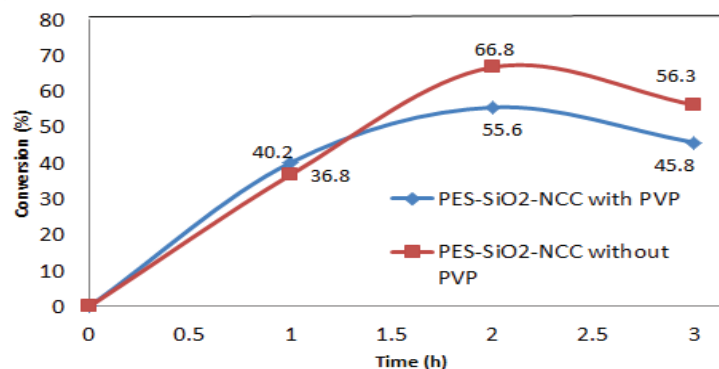


FIGURE 3. The effect of PVP K30 on the enzymatic production of pentyl valerate catalyzed by CRL/PES-SiO₂-NCC in 3 h of reaction [Temperature: 50 °C, Enzyme loading: 3 mg/mL, molar ratio acid: alcohol 1:2, 200 rpm]

Effect of Percentage of SiO₂-NCC Nanoparticles

The effect of the amount of added SiO₂-NCC nanoparticles into the PES membrane was also evaluated. The number of nanoparticles in the membrane was investigated between 0.1–5% (w/w) (Figure 4). Data showed enhanced pentyl valerate production catalyzed by CRL/PES-SiO₂-NCC with increasing amounts of incorporated SiO₂-NCC nanoparticles. A 5.0% addition of SiO₂-NCC gave the highest percent conversion of the ester at 78.3%, followed by 3.0% SiO₂-NCC (62.2%) and SiO₂-NCC at 1.5% and 0.1% that yielded 62% and 48.2% of the ester, respectively.

The trend seen here indicated that the higher presence of SiO₂-NCC nanoparticles in the composite enhanced activity of CRL and resulted in higher yields of pentyl valerate. A possible reason for this was because of the abundance of hydroxyl groups on the surface of SiO₂-NCC, that led to the slight increase in hydrophilicity of the composite [25]. It is worth highlighting here that the correct balance of hydrophobic/hydrophilic in the developed PES-SiO₂-NCC composite is a key feature to consider. Studies have shown that a certain degree of hydrophobicity is required to stabilize the hydrophobic lid of CRL into its open form to ensure direct entry of substrates into the lipase active site [26, 27]. On the other hand, the presence of hydrophilic hydroxyl groups on the surface of NCC improves the reactivity of the component in a chemical reaction. The incorporation of NCC into the composite can promote more intermolecular hydrogen bonds with SiO₂, while hydrogen bonds are formed between the –OH groups of SiO₂-NCC with the S=O belonging to PES. Such intermolecular interactions are useful for increasing robustness of the resultant hybrid composite during mechanical stirring, and as expected, provided an excellent biocompatible surface for CRL immobilization and activation. Thereby, the resultant immobilized lipase was capable of producing higher yields of pentyl valerate.

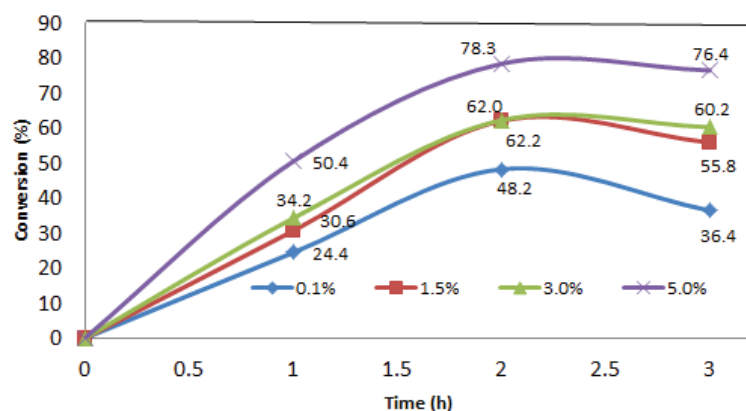


FIGURE 4. Effect of the percentage of nanoparticles on the enzymatic production of pentyl valerate catalyzed by CRL/PES-SiO₂-NCC in 3 h of reaction [Temperature: 50 °C, Enzyme loading: 3 mg/mL, molar ratio acid: alcohol 1:2, 200 rpm]

Effect of Composite Size

The effect of composite size on the enzymatic production of pentyl valerate was assessed, and the results are presented in Figure 5. The highest conversion of pentyl valerate was achieved when using CRL/PES-SiO₂-NCC of size 0.02 cm (76.4%), while the lowest yield was observed for CRL/PES-SiO₂-NCC (34.2%) of 2 cm, within 2 h reaction duration. The results obtained here agreed with the reported use of smaller structures facilitating reduced diffusional restriction of the particulates, as well as providing a higher functional surface area [28]. Having said that, this indirectly permitted higher immobilization efficiency of the CRL, thereby yielding higher conversion degree of the ester. Contrariwise, the largest CRL/PES-SiO₂-NCC composite (2 cm) gave the lowest yield can be ascribed to the lower available surface area for attachment that limited access of the triglyceride molecules in the esterification reaction [29]. The study demonstrated the importance of using a correct membrane size for lipase immobilization, as to ensure efficient production of pentyl valerate. The 0.02 cm composite size was shown to be optimal to support the highest yield of the ester, likely because of the highest number of available surface area for the CRL to interact with the substrates.

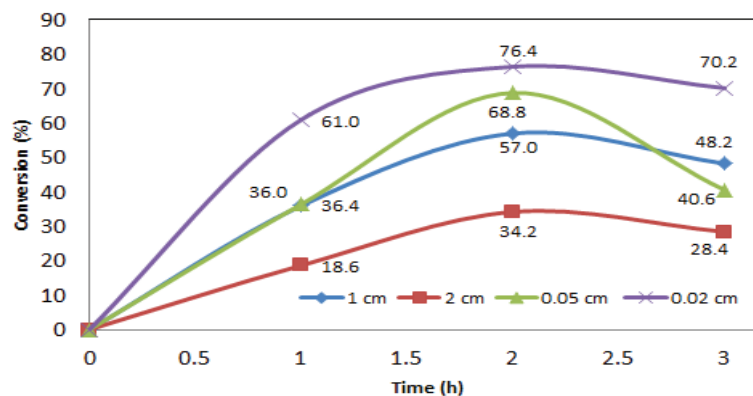


FIGURE 5. The effect of composite size on the enzymatic production of pentyl valerate catalyzed by CRL/PES-SiO₂-NCC in 3 h of reaction [Temperature: 50 °C, Enzyme loading: 3 mg/mL, molar ratio acid: alcohol 1:2, 200 rpm]

CONCLUSION

We demonstrated that the SiO₂ and NCC nanoparticles isolated from pretreated OPFL were prospective components for reinforcement of PES membrane for the immobilization and activation of CRL for enhanced pentyl valerate production. FTIR: ATR spectral data of SiO₂-NCC indicated that NCC was hydrogen-bonded to SiO₂ while XRD diffractograms successfully revealed the crystalline nature of extracted SiO₂ and NCC. Pertinently, the best condition to fabricate PES-SiO₂-NCC for CRL immobilization required the use of

CRL/PES-SiO₂-NCC with pore former, composite size of 0.02 cm and 5% w/w percentage of nanoparticles. A maximum yield of pentyl valerate of 78.3% was attained after 2 h of reaction under these process parameters to prepare the hybrid composite. The resultant hybrid composite activated CRL activity, as well as yielded a more robust enzyme for efficient esterification production of pentyl valerate.

ACKNOWLEDGMENTS

This work supported by the Fundamental Research Grant Scheme from the Ministry of Higher Education Malaysia (Q.J130000.2526.17H48).

REFERENCES

1. T. Raghavendra, N. Panchal, J. Divecha, A. Shah, and D. Madamwar, *BioMed Res. Int.* 2014, (2014).
2. J. Tao and J.-H. Xu, *Curr. Opin. Chem. Biol.* **13**, 43-50 (2009).
3. S.M. Thomas, R. DiCosimo, and V. Nagarajan, *Trends Biotechnol.* **20**, 238-242 (2002).
4. R. Saxena, A. Sheoran, B. Giri, and W.S. Davidson, *J. Microbiol. Methods* **52**, 1-18 (2003).
5. A. Houde, A. Kademi, and D. Leblanc, *Appl. Biochem. Biotechnol.* **118**, 155-170 (2004).
6. N.H.C. Marzuki, N.A. Mahat, F. Huyop, H.Y. Aboul-Enein and R.A. Wahab, *Food and Bioprod. Process.* **96**, 211-220 (2015).
7. I.N.A. Rahman, N. Attan, N.A. Mahat, J. Jamalis, A.S.A. Keyon, C. Kurniawan and R.A. Wahab, *Int. J. Biol. Macromol.* **115**, 680-695 (2018).
8. P. Zucca and E. Sanjust, *Molecules* **19**, 14139-14194 (2014).
9. I.B.-B. Romdhane, Z.B. Romdhane, A. Gargouri, and H. Belghith, *J. Mol. Catal. B: Enzym.* **68**, 230-239 (2011).
10. C. Mateo, J.M. Palomo, G. Fernandez-Lorente, J.M. Guisan and R. Fernandez-Lafuente, *Enzyme Microb. Technol.* **40**, 1451-1463 (2007).
11. A. Mishra and S. Ghosh, *Fuel* **236**, 544-553 (2019).
12. K. Raj and C. Krishnan, *Ind. Crop Prod.* **131**, 32-40 (2019).
13. E. Onoja, S. Chandren, F.I.A. Razak and R.A. Wahab, *J. Biotechnol.* **283**, 81-96 (2018).
14. F. Beltramino, M.B. Roncero, A.L. Torres, T. Vidal and C. Valls, *Cellulose* **23**, 1777-1789 (2016).
15. A.G. de Souza, D.B. Rocha, F.S. Kano and D. dos Santos Rosa, *Resour. Conserv. Recy.* **143**, 133-142 (2019).
16. M.M. Haafiz, A. Hassan, Z. Zakaria and I. Inuwa, *Carbohydr. Polym.* **103**, 119-125 (2014).
17. D. Datta and G. Halder, *J. Polym. Environ.* 1-18 (2019).
18. M. Naddaf, H. Kafa and I. Ghanem, *Silicon* 1-8 (2019).
19. L. Segal, J. Creely, A. Martin Jr and C. Conrad, *Text. Res. J.* **29**, 786-794 (1959).
20. F.I. Ditzel, E. Prestes, B.M. Carvalho, I.M. Demiate and L.A. Pinheiro, *Carbohydr. Polym.* **157**, 1577-1585 (2017).
21. A.W.T. Owolabi, G. Arniza, W. wan Daud, and A.F. Alkharkhi, *BioResources* **11**, 3013-3026 (2016).
22. R.M. Sheltami, I. Abdullah, I. Ahmad, A. Dufresne and H. Kargazadeh, *Carbohydr. Polym.* **88**, 772-779 (2012).
23. E.K. Pasandideh, B. Kakavandi, S. Nasser, A.H. Mahvi, R. Nabizadeh, A. Esrafil, and R.R. Kalantary, *J. Environ. Health Sci.* **14**, 21 (2016).
24. B. Vatsha, J.C. Ngila, and R.M. Moutloali, *Phys. Chem. Earth* **67**, 125-131 (2014).
25. M. Subramaniam, P. Goh, W. Lau, Y. Tan, B. Ng and A. Ismail, *Chem. Eng. J.* **316**, 101-110 (2017).
26. M. Aghababae, M. Beheshti, A.-K. Bordbar and A. Razmjou, *RSC Adv.* **8**, 4561-4570 (2018).
27. N. Pujari, B. Vaidya, S. Bagalkote, S. Ponrathnam, and S. Nene, *J. Membrane Sci.* **285**, 395-403 (2006).
28. T. Xie, A. Wang, L. Huang, H. Li, Z. Chen, Q. Wang and X. Yin, *Afr. J. Biotechnol.* **8**, (2009).
29. A. Anand and L.R. Weatherley, *Process Biochem.* **68**, 100-107 (2018).